Breakdown of Feynman scaling law and cosmic-ray exotic events

Akinori Ohsawa
Institute for Cosmic Ray Research, University of Tokyo, Tanashi, Tokyo 188, Japan

Kotaro Sawayanagi
Instituto de Fisica Gleb Wataghin, Universidade Estadual de Campinas, 13081 Campinas, Sao Paulo, Brazil
(Received 29 August 1991)

The breakdown of the Feynman scaling law, observed at the CERN SPS $\bar{p}p$ collider ($\sqrt{s}=540$ or 900 GeV), leads to decreasing inelasticity, which is not compatible with high-energy cosmic-ray data ($E_0=10^{14}-10^{16}$ eV) obtained through emulsion-chamber experiments. It is pointed out that the existence of the cosmic-ray exotic events of Centauro, Chiron, etc., possibly reconciles the discrepancy.

PACS number(s): 13.85.Tp, 13.85.Hd

I. INTRODUCTION

Cosmic-ray exotic events (Centauro, Chiron, etc.) [1,2], reported by the Chacaltaya emulsion-chamber experiment, have attracted great interest, and many speculations were proposed on their origin [3]. It is important to decide the issue of them because their existence is one of the challenges to the standard model. Experimentally, the statistics on candidate events is increasing steadily through emulsion-chamber experiments. However, they are not in the situation to be accepted widely. It is partly because cosmic-ray experiments (by emulsion chamber) have inevitable vulnerable points, such as (1) ambiguities due to unknown parameters, proper to cosmic-ray experiments, (2) noncomprehensive observation, and (3) scarce intensity of exotic events, though this is almost the unique way to study them. Hence, in the present paper, we will try to make a cross check on the exotic events, which is crucial for cosmic-ray experiments.

Recently accelerators have reached energies high enough to compare, directly, i.e., without extrapolation into a higher-energy region, their data on multiple-particle production with those by cosmic-ray experiments. And it was found that both sets of data are quite consistent with each other. That is, the C-jet data of the Chacaltaya emulsion-chamber experiments [4] are (re)confirmed by the experiments of the CERN SPS $\bar{p}p$ collider [5]. C jets are the direct observation of γ rays produced in multiple-particle productions which occur in the built-in target in the two-storied emulsion chamber. Their interaction energies are between 10^{14} and 10^{15} eV, which just corresponds to an energy of the CERN collider of $\sqrt{s}=540$ or 900 GeV. The confirmation is with respect to the increase of the rapidity density, the increase of average p_T, the correlation between the rapidity density and average p_T, the existence of jet structure, etc., all of which were pointed out already in the early 1980s through C-jet experiments [4].

Among the conclusions of emulsion-chamber experiments, however, there are important points which have remained without confirmation by accelerator experiments. Those are the breakdown of the Feynman scaling law in the forward region [4,6] and the existence of exotic events. As to the former, most who are interested in multiple-particle production are still believing it holds, and as to the latter, the search for Centauro events through accelerators has resulted in none found [7].

In our previous paper [8], we pointed out that the scaling law, appearing to hold in the low-energy region of $\sqrt{s}<60$ GeV [9], breaks down distinctly in the high-energy region of $\sqrt{s}=540-900$ GeV by constructing the empirical formula of a rapidity density distribution in the energy region of $\sqrt{s}=10-900$ GeV. The same conclusion was also found by Wdowczyk and Wolfendale [10]. And we also pointed out that the scale-breaking feature may relate closely to the existence of cosmic-ray exotic events by comparing its consequences with cosmic-ray data. That is, cosmic-ray data by emulsion-chamber experiments, which reflect the nuclear interactions in $10^{14}-10^{16}$ eV, are not compatible with the observed scale-breaking feature which resulted in decreasing inelasticity, but rather are consistent with the scaling feature. One of the ways to reconcile the contradictory situation is to introduce another component—the decay into "h particles" (probably hadrons except pions), in the forward region of multiple-particle production. The production of the component in the forward region, responsible for exotic events, can compensate for the decrease in inelasticity and also explain why Centauro searches were in vain.

Our previous work, however, contained several points to be improved. Those are (1) the experimental data of the rapidity density distribution, collected by the UA5 Collaboration at the CERN collider, are available in the central region of $|y^*|<5.0$, but not in the forward region; (2) p_T is assumed to be constant over y^* in converting $d\sigma/dy^*$ to $d\sigma/dx$, necessary for the analysis; and (3) the calculation to relate the cosmic-ray observation with the features of multiple-particle production involves approximations which should not be neglected.

Afterwards there has been progress in the following points. As to (1) and (2), the UA7 Collaboration obtained the rapidity density and p_T in the forward region, and as to (3) we got the improved solutions of the diffusion equa-

tions of cosmic-ray components in the atmosphere. So, in the present paper, we will examine the validity of the previous conclusions in Ref. [8] on the improved material. The form of the paper is to examine the data by accelerator experiments in Sec. II, to examine the cosmic-ray data in Sec. III, and to have a discussion in Sec. IV.

II. SCALE-BREAKING FEATURE IN MULTIPLE-PION PRODUCTION

A. Data from the UA5 Collaboration

According to Ref. [8], the rapidity density distributions of charged particles in inelastic events at energies of $\sqrt{s}=53$, 200, 540 and 900 GeV, obtained by the UA5 Collaboration at the CERN collider [11], can be reproduced well by

$$\frac{1}{\sigma_{\text{inel}}}\frac{d\sigma}{dy^*}=A\left[\frac{s}{s_0}\right]^{\alpha}\left[1-\left[\frac{s}{s_0'}\right]^{\alpha'}\frac{p_T}{\sqrt{s}}e^{y^*}\right]^4, \tag{2.1}$$

where $A=1.67$, $\alpha=0.11$, $\alpha'=0.26$, $s_0=6.3\times10^2$ GeV^2, $s_0'=3.4\times10^3$ GeV^2, and $p_T=0.4$ GeV/c. Using the relation between x $(=E/E_0)$ and y^*,

$$x\cong x^*\cong\frac{p_T}{\sqrt{s}}e^{y^*}, \tag{2.2}$$

where the asterisk is for the quantities in the c.m. system (c.m.s.), we have, for Eq. (2.1),

$$\frac{1}{\sigma_{\text{inel}}}\frac{d\sigma}{dx}=A\left[\frac{s}{s_0}\right]^{\alpha}\left[1-\left[\frac{s}{s_0'}\right]^{\alpha'}x\right]^4\frac{1}{x}. \tag{2.3}$$

It should be noted that $p_T=0.4$ GeV/c is assumed independently of y^*. The formula shows that the scaling law of

$$\frac{1}{\sigma_{\text{inel}}}\frac{d\sigma}{dx}=A(1-x)^4\frac{1}{x}, \tag{2.4}$$

which is one of the expressions of the scaling function, established in the low-energy region of bubble-chamber experiments, breaks down at high energy in the forward region as well as in the central region.

B. Data from the UA7 Collaboration

The UA7 Collaboration [12] got the rapidity density and the average p_T of π^0's in the forward region at $\sqrt{s}=630$ GeV. The rapidity density is consistent with Eq. (2.1) [13], which is constructed empirically from the data in the central region.

From UA7 data we can construct the x distribution directly without assuming constant p_T. That is, by Eq. (2.2) we have

$$x\frac{d\sigma}{dx}=\frac{d\sigma}{dy^*}\frac{1}{1+d(\ln p_T)/dy^*}, \tag{2.5}$$

where $d(\ln p_T)/dy^*=-0.4$ in the forward region from UA7 data.

Figure 1 shows the x distribution of charged particles, constructed from UA7 data by Eq. (2.5), where

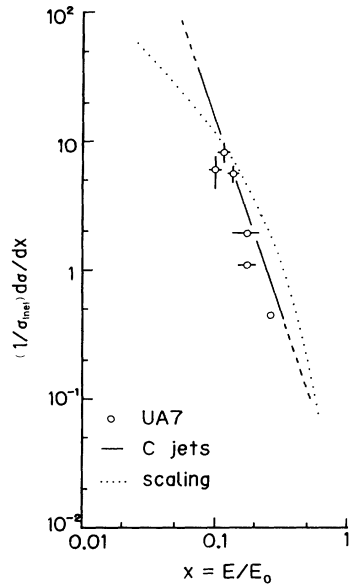

FIG. 1. Energy spectrum of produced particles (charged) in terms of x $(=E/E_0)$. Open circles are constructed from UA7 data ($\sqrt{s}=630$ GeV) of rapidity density and p_T of π^0's, assuming $\sigma_{\text{inel}}=49.0$ mb and $\pi^{\pm}/\pi^0=2.0$. The straight line is by C jets ($\langle\sqrt{s}\rangle=500$ GeV), the solid line corresponds to the region where the experimental data exist. The dotted curve is the scaling function of Eq. (2.4) in the text. The former two agree well with each other and stand apart from the scaling function.

$\sigma_{\text{inel}}=49.0$ mb and $\pi^{\pm}/\pi^0=2.0$ are assumed. One of the C jets and the scaling distribution of Eq. (2.4) are also shown together. The data of UA7 and C jets agree well with each other[1] and stand apart from the scaling function, indicating scale breaking.[2]

Fitting Eq. (2.3) to the data of UA7 in Fig. 1, one finds

$$\begin{aligned}&A=1.67,\\&\alpha=0.11,\\&\alpha'=0.17,\\&s_0=6.3\times10^2\ \text{GeV}^2,\end{aligned} \tag{2.6}$$

and

$$s_0'=1.8\times10^3\ \text{GeV}^2$$

in Eq. (2.3), which indicate scale breaking still, though the s dependence becomes weaker than in Eq. (2.3), owing to the y^* dependence of p_T. And the consequent inelasticity, obtained by assuming that all the produced particles are pions, is

$$K(E)=\frac{3}{2}A\left[\frac{s}{s_0}\right]^{\alpha}\left[\frac{s}{s_0'}\right]^{-\alpha'}\frac{1}{5}=0.5\left[\frac{E}{E_K}\right]^{-\kappa}, \tag{2.7}$$

[1]Data of the C jets were confirmed by the accelerator experiment on this point too.

[2]The UA7 Collaboration concludes the validity of the Feynman scaling law in terms of $d\sigma/dy^*$ instead of $1/\sigma_{\text{inel}}d\sigma/y^*$.

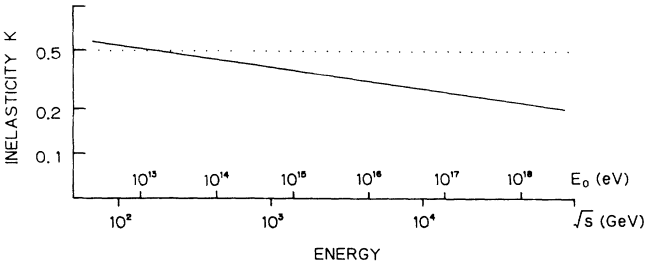

FIG. 2. Energy dependence of inelasticity obtained from the empirical formula to fit the UA7 data in Fig. 1.

where $\kappa=\alpha'-\alpha=0.06$ and $E_K=5.2\times10^3$ GeV, showing a decrease with energy (Fig. 2).

C. Scale breaking in pion multiple production

We see that x distributions of produced particles, by UA7 and C jets, which agree well with each other, show a scale-breaking feature in the forward region. We should keep in mind, however, that the data of both experiments concern only π^0's among produced particles.

III. SCALE-HOLDING FEATURE BY COSMIC-RAY DATA

It is interesting to examine how the scale-breaking feature is in the nuclear interactions of still higher-energy regions, where the characteristics become more distinct, by observing nuclear interactions induced by cosmic rays. The direct observation of nuclear interactions in the energy region exceeding 10^{15} eV, however, is not easy due to the scarce intensity of cosmic rays, and we have to observe the nuclear interactions in the atmosphere by the detectors installed at high mountains.

To observe the high-energy cosmic-ray events in detail, the emulsion chamber is the most suitable detector, and experiments have been carried out at various altitudes of balloons, airplanes, and high mountains.

In the present work we examine the intensity of electromagnetic (em) component, i.e., electrons ($e^{\pm}$) and photons, observed by emulsion-chamber experiments. The experimental data are to be compared with the calculation in which the scale-breaking feature is taken into account.

A. Emulsion chamber (EC)

The EC, a multilayered sandwich of lead plates and photosensitive layers (nuclear emulsion plates and/or x-ray films), is sensitive to electron showers, which are produced in the chamber either by an em component or by a hadronic component of high energy (of shower energy exceeding 1 TeV). It is possible to determine their energies and positions with a high precision of $\Delta E/E=20\%$ and $\Delta x=10\ \mu$m, respectively [1].

B. Diffusion of cosmic-ray components in the atmosphere

A primary cosmic ray of high energy, plunging into the atmosphere, collides with the atmospheric nucleus to produce secondary particles of hadronic and em components. The former [including surviving nucleon(s)] cause nuclear interactions again. On the other hand, the em components (mainly through $\pi^0\rightarrow2\gamma$) produce themselves through em interaction. These processes repeat themselves successively in the atmosphere.

The diffusion of cosmic rays in the atmosphere, described above, is solved semianalytically, details of which are given in the Appendix. We list here the basic assumptions necessary for the calculation.

(i) Energy spectrum of primary cosmic rays. We assume, for the energy spectrum of primary cosmic rays in integral form,

$$I(E,0)=N_0\left[\frac{E}{E_c}\right]^{-\gamma}, \tag{3.1}$$

where $\gamma=1.8$. Our discussion is made free from the absolute value of the intensity.

(ii) Energy spectrum of produced particles. Rewriting Eq. (2.6) by the quantities in the laboratory system

$$\psi(E_0,E)=A\left[\frac{E_0}{E_s}\right]^{\alpha}\left[1-\left[\frac{E_0}{E_s'}\right]^{\alpha'}\frac{E}{E_0}\right]^4\frac{1}{E}, \tag{3.2}$$

where $E_s=3.4\times10^2$ GeV and $E_s'=9.6\times10^2$ GeV. And we assume that all the produced particles are pions.

(iii) Inelasticity. We will examine the case of $\kappa=0.06$ and 0 in Eq. (2.7), though the former case corresponds to the energy spectrum of Eq. (3.2). This is because the former case is not compatible with cosmic-ray data, as can be seen later. The meaning of the latter case will be discussed in Sec. IV.

In the calculation the inelasticity is assumed to have a uniform distribution between 0 and 2 $K(E)$, which leads to $K(E)$ for the average value.

(iv) Mean free path (mfp) of nucleons in the air. The cross section of the nucleon-air collision is assumed to increase with energy in the same manner as that of pp does. Correspondingly the mfp of nucleons in the air is assumed to be

$$\lambda_N(E)=\lambda_N\left[\frac{E}{E_c}\right]^{-\beta}, \tag{3.3}$$

where $\lambda_N=80.0$ g/cm^2, $E_c=2.0\times10^2$ GeV, and $\beta=0.06$.

(v) Only the nucleon collisions to be considered. The em components are produced by both the nucleon and pion collisions. The latter process, however, is neglected in the calculation because the energy spectrum of our concern is the scale-breaking one.

C. Comparison with cosmic-ray data

Figure 3 shows the altitude dependence of cosmic-ray intensity (in integral form) of em components for the cases of $\kappa=0.06$ and 0. The "scaling" case of $\alpha=\alpha'=\beta=0$ (and, consequently, $\kappa=0$), which means assuming the scaling type of production spectrum and an energy-independent mfp, and for which the analytic solutions are possible, is shown together for comparison. Experimental data ($E=5$ TeV) by the EC experiments are

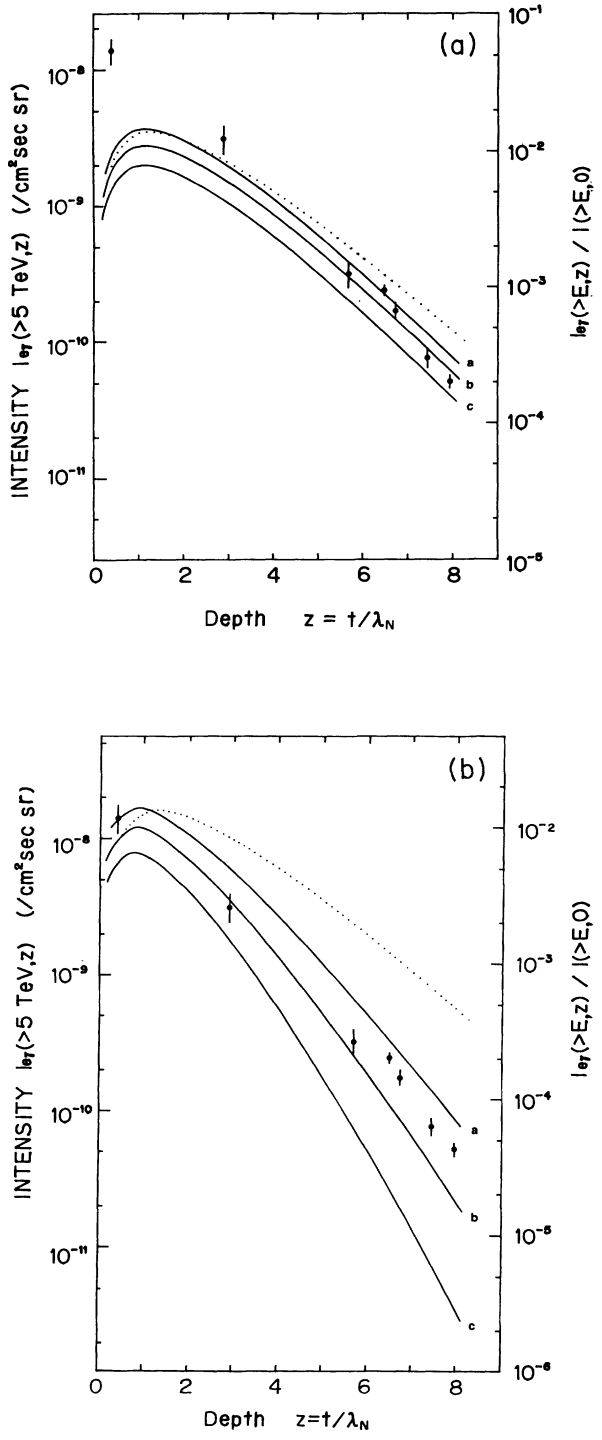

FIG. 3. Altitude dependence of cosmic-ray intensity (in integral form) of electromagnetic component. Solid curves are the calculation where the scale-breaking feature is taken into account, and the letters *a*, *b*, and *c*, attached to them, signify the energies of $E=1$, 10, and 10^2 TeV, respectively. (a) and (b) correspond to the cases of $\kappa=0.06$ (the decreasing inelasticity) and $\kappa=0$ (the constant inelasticity of 0.5). The dotted curve of "scaling" case is also shown together for comparison. (See the text.) The data ($E=5$ TeV) are by emulsion-chamber experiments at various altitudes of balloons, airplanes, and high mountains.

at various altitudes of balloons, airplanes, and high mountains. Remarks on the data are given in Ref. [8].

Figure 3(a) shows that the altitude dependence in the case of $\kappa=0.06$ cannot reproduce the experimental data, giving a longer attenuation of the mfp than the experiments. This long attenuation of the mfp, which is similar to the one in the "scaling" case, is due to the cancellation of the two effects of nucleons: the scale-breaking feature (lengthening mfp through decreasing inelasticity) and the increasing cross section (shortening it). On the other hand, Fig. 3(b) shows that the case of $\kappa=0$ reproduces the experimental data quite well, indicating that the inelasticity is $K=0.5$ independently of energy.

IV. DISCUSSION

(1) The intensity of the em component is the most suitable to be compared with the calculation among those observed by EC experiment in the following sense.

(i) The em component can be collected efficiently and identified easily by the EC, compared with the hadronic component, and those energies are determined directly by the EC without any assumptions.

(ii) Intensity is a well-defined quantity, free from the selection bias, and therefore the data by different experiments can be compared directly.

(iii) Use of the data of independent experiments at various altitudes makes the analysis free from the systematic bias which each experiment may involve.

And our analysis is free from the absolute value of intensity, which depends heavily on the absolute value of energy.

(2) Comparison of accelerator data in the low-energy region ($\sqrt{s}<30$ GeV by bubble-chamber experiments) and in the high-energy region ($\sqrt{s}=540$ and 900 GeV by the CERN $\bar{p}p$ collider SPS) shows clearly the breakdown of the Feynman scaling law in the forward region as well as in the central region in terms of $1/\sigma_{\text{inel}} d\sigma/dx$. It should be noted that the above statement is valid only for π^0's and, consequently, for pions among produced particles.

(3) The x distribution of the scale-breaking feature, constructed empirically from the accelerator data, brings about the decreasing inelasticity with energy. It, however, is not compatible with the cosmic-ray data which reflect the nuclear interactions in the energy region of 10^{14}–10^{16} eV. That is, the intensity of the em component, observed by EC experiments at various altitudes, shows a much shorter attenuation of the mfp than that by the calculation in which the decreasing inelasticity is taken into account, being rather consistent with the case of energy-independent inelasticity.

(4) The discrepancy between the decreasing inelasticity (concluded by accelerator experiments and also the cosmic-ray experiments of C jets) and the constant inelasticity (by cosmic-ray experiments) can be reconciled by introducing another component (the decay into "h particles") in the forward region. Production of the component compensates the discrepancy.

h particles cannot be pions because π^0's (or γ rays) in the forward region are shown to be consistent with the

scale-breaking distribution, as discussed in Sec. II, and therefore have attributes similar to those observed in cosmic-ray exotic events. It also explains why Centauro searches were negative by the collider-type accelerators.

The production of some exotic component in the forward region is also discussed by several authors in relation with cosmic-ray exotic events [14,15].

(5) The existence of exotic events is also suggested by another type of cosmic-ray experiment, the Fly's Eye experiment [16], which is due to Ellis *et al.* in relation to their model of multiple-particle production [15]. The Fly's Eye experiment observes the profile of extensive air showers produced by cosmic-ray nuclei with energies above 10^{17} eV through the measurement of atmospheric nitrogen fluorescence light. The depth of the shower maximum, $X_{\max}$, is significantly smaller than expected on the basis of existing simulations of showers initiated by primary protons, but consistent with the simulations of showers initiated by nuclei such as iron. On the other hand, the observed variation in $X_{\max}$ is in good agreement with simulations of proton-induced showers. Those features are quite consistent with the production of exotic events by protons.

(6) Our discussion so far concerns the inclusive spectrum of produced particles. Hence, it is not necessary for ordinary particles and h particles to coexist in one event of multiple-particle production, and it is the case in cosmic-ray exotic events. Following this scenario, we can estimate the branching ratio (p) of the h-particle production (Fig. 4) by

$$K_{\text{tot}}=(1-p)K(E)+pK_h \ , \tag{4.1}$$

where $K_{\text{tot}}=0.5$ and $K_h=1.0$ are assumed. The branching ratio becomes appreciable in the energy region of $E\geq 10^{15}$ eV with the probability of $\geq 20\%$, which is consistent with the cosmic-ray observation of exotic events, i.e., one event per 100 m^2 y of exposure.

(7) In conclusion, although the revised formula of the secondary particle distribution differs slightly from the previous one, it is not necessary to revise our previous conclusion at all. We did not try to specify the characteristics of h particles in this work because we need to define the high-energy pion interaction in detail. Therefore, for our purpose, it is better to observe the events directly by experiment.

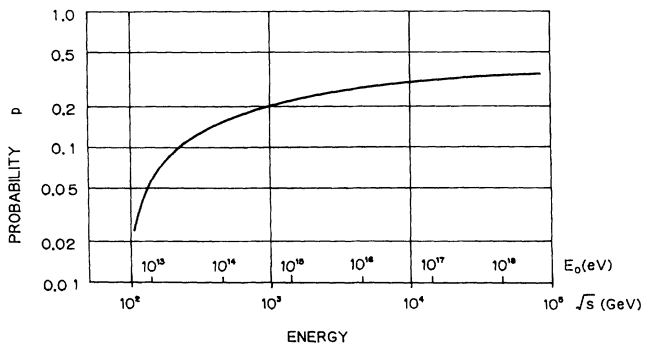

FIG. 4. Branching ratio of h-particle production channel, assuming the scenario that ordinary multiple-particle production (of decreasing inelasticity with energy) and h-particle production conspire to bring the energy-independent inelasticity of 0.5 on average.

ACKNOWLEDGMENTS

The authors thank the members of the Chacaltaya Emulsion Chamber Experiment of the Brasil-Japan Collaboration for their valuable discussions and comments. One of us (K.S.) also thanks FAPESP of São Paulo, in Brazil, for financial support (Processo No. 89/3870-5) for him to stay in Japan because the initial stage of the present work started there.

APPENDIX: DIFFUSION OF COSMIC-RAY COMPONENTS IN THE ATMOSPHERE

We will describe briefly the diffusion equations of cosmic-ray components in the atmosphere and their solutions because those are given in detail in Ref. [8]. Our concern is with respect to hadronic (nucleonic and pionic) and electromagnetic components, whose differential energy spectrum is expressed by

$$F_i(E,t)dE \quad (i=N,\ \pi,\ \text{and em}) \ , \tag{A1}$$

where t is the depth in the atmosphere.

1. Nucleonic component

The diffusion equation is

$$\frac{\partial F_N}{\partial t}=-\frac{F_N(E,t)}{\lambda_N(E)} + \int \delta(E-(1-K)E_0)\frac{F_N(E_0,t)}{\lambda_N(E_0)}dE_0\,dK \ . \tag{A2}$$

By Mellin transformation Eq. (A2) turns into

$$\frac{\partial f_N}{\partial z}=-\hat{\beta}f_N(s,z)+\frac{1}{s+1}\left[\frac{E_c}{E_K}\right]^{\kappa}\hat{\delta}f_N(s,z) \ , \tag{A2'}$$

where the operators $\hat{\beta}$ and $\hat{\delta}$ have the functions of

$$\hat{\beta}f(s)=f(s+\beta) \ ,$$

$$\hat{\delta}f(s)=f(s+\beta+\kappa) \ ,$$

and $z=t/\lambda_N$. Equation (A2 ′) can be solved easily as

$$f_N(s,z)=e^{-\Lambda z}\sum\frac{z^n}{n!}[\Lambda-\hat{\beta}+\mu_N(s)\hat{\delta}]^n f_N(s,0) \ , \tag{A3}$$

where $f_N(s,0)$ is the intensity of nucleonic component at the top of the atmosphere, which is given by Eq. (3.1), i.e.,

$$f_n(s,0)=\frac{\gamma}{s-\gamma}[(E_0/E_c)^{s-\gamma}-1] \quad (E_0=10^8\ \text{GeV}) \tag{A4}$$

and

$$\mu_N(s)=\frac{1}{s+1}(E_c/E_K)^{\kappa} \ . \tag{A5}$$

2. Electromagnetic component

Following assumption (v) in Sec. III B, the em component is expressed by

$$F_{\rm em}(E,z)=\int_0^z dt\int_E^\infty dE_0(\pi+\gamma)(E_0,E,z-t)P_\gamma(E_0,t)\ . \tag{A6}$$

The first term in the integrand is the number of electrons and photons, produced by a primary photon of energy E_0, and given by

$$(\pi+\gamma)(E_0,E,z)=\frac{1}{2\pi i}\int\frac{ds}{E}\left[\frac{E_0}{E}\right]^s N_i(s)e^{\lambda_i(s)z}\ , \tag{A7}$$

and the second is the production spectrum of photons, given by

$$P_\gamma(E,z)=\int_E^\infty\frac{2}{E'}dE'\int_{E_{0(\min)}}^\infty dE_0\frac{1}{2}\psi(E_0,E')\frac{F_N(E_0,z)}{\lambda_N(E_0)}\ . \tag{A8}$$

Mellin transforms of Eqs. (A6) and (A8) are given by

$$f_{\rm em}(s,z)=\int_0^z dt\,N_i(s)e^{\lambda_i(s)(z-t)}p_\gamma(s,t)\ , \tag{A6'}$$

$$p_\gamma(s,z)=\frac{1}{s+1}\psi(s)\hat{\alpha}f_N(s,z)\ , \tag{A8'}$$

where

$$\psi(s)=(E_c/E_s)^\alpha(E_c/E_s')^{-\alpha'}\phi(s)\ , \tag{A9}$$

$$\phi(s)=\int_0^1 x^s dx\ A\frac{(1-x)^4}{x} \tag{A10}$$

and

$$\hat{\alpha}f(s)=f((1-\alpha')s+\alpha+\beta)\ .$$

An inverse Mellin transformation, defined by

$$I_{\rm em}(E,z)=\frac{1}{2\pi i}\int\frac{ds}{s}\left[\frac{E_c}{E}\right]^s f_{\rm em}(s,z)\ , \tag{A11}$$

which can be evaluated by the saddle-point method, gives the intensity (in integral form) of the cosmic-ray component at the depth z.

[1] C. M. G. Lattes, Y. Fujimoto, and S. Hasegawa, Phys. Rep. **65**, 152 (1980).

[2] S. Hasegawa, Institute for Cosmic Ray Research, University of Tokyo, Report No. 151-87-5 (unpublished).

[3] For example, J. D. Bjorken and L. D. McLerran, Phys. Rev. D **20**, 2353 (1979); E. Witten, *ibid.* **30**, 272 (1984).

[4] Chacaltaya Emulsion Chamber Collaboration, J. A. Chinellato *et al.*, Prog. Theor. Phys. Suppl. **76**, 1 (1983); H. Kumano, *ibid.* **76**, 51 (1983).

[5] J. Rushbrook, CERN Report No. CERN-EP/85-178, 1985 (unpublished); F. Halzen, P. Hoyer, and N. Yamdagni, Phys. Lett. B **190**, 211 (1987).

[6] N. Arata, Nucl. Phys. **B211**, 189 (1983); T. Tabuki, Prog. Theor. Phys. Suppl. **76**, 40 (1983).

[7] UA1 Collaboration, G. Arnison *et al.*, Phys. Lett. **122B**, 189 (1983); UA5 Collaboration, G. J. Alner *et al.*, CERN Report No. CERN-EP/86-127, 1986 (unpublished); UA5 Collaboration, K. Alpgard *et al.*, Phys. Lett. **115B**, 71 (1982).

[8] J. Bellandi F., S. Q. Brunetto, J. A. Chinellato, C. Dobrigkeit, A. Ohsawa, K. Sawayanagi, and E. H. Shibuya, Prog. Theor. Phys. **83**, 58 (1990).

[9] F. E. Taylor, D. C. Carey, J. R. Johnson, R. Kammerud, D. J. Richie, A. Roberts, J. R. Sauer, R. Shafer, D. Theriot, and J. K. Walker, Phys. Rev. D **14**, 1217 (1976).

[10] J. Wdowczyk and A. W. Wolfendale, Nuovo Cimento **54A**, 433 (1979); J. Phys. G **10**, 257 (1984); **13**, 411 (1987).

[11] UA5 Collaboration, G. J. Alner *et al.*, CERN Report No. CERN-EP/86-126, 1986 (unpublished); Z. Phys. C **33**, 1 (1986).

[12] E. Pare, T. Doke, M. Haguenauer, V. Innocente, K. Kasahara, T. Kashiwagi, J. Kikuchi, S. Lanzano, K. Masuda, H. Murakami, Y. Muraki, T. Nakada, A. Nakamoto, and T. Yuda, CERN Report No. CERN-EP/89-181, 1990 (unpublished); Phys. Lett. B **242**, 531 (1990).

[13] A. Ohsawa, Prog. Theor. Phys. **84**, 55 (1990).

[14] K. Goulianos, Rockefeller University Report No. RU 81/A 98, 1981 (unpublished); K. Kang and A. R. White, Argonne National Laboratory Report No. ANL-HET-PR-90-12, 1990 (unpublished).

[15] J. Ellis, M. Karliner, and D. N. Schramm, Phys. Lett. B **252**, 282 (1990).

[16] G. L. Cassiday, R. Cooper, S. C. Carbato, B. R. Dawson, J. W. Elbert, B. E. Fick, K. D. Green, D. B. Kieda, S. Ko, D. F. Liebing, E. C. Loh, M. H. Salamon, J. D. Smith, P. Sokolsky, P. Sommers, S. B. Thomas, S. X. Wang, and B. Wheeler, Astrophys. J. **356**, 669 (1990).